Full Paper

Wiley Online Library

ELECTROANALYSIS

DOI: 10.1002/elan.202000032

A Biosilification Fusion Protein for a 'Self-immobilising' Sarcosine Oxidase Amperometric Enzyme Biosensor

Si Chen[a] and Elizabeth A. H. Hall*[a]

Abstract: Monomeric sarcosine oxidase (mSOx) fusion with the silaffin peptide, R5, designed previously for easy protein production in low resource areas, was used in a biosilification process to form an enzyme layer electrode biosensor. mSOx is a low activity enzyme (10–20 U/mg) requiring high amounts of enzyme to obtain an amperometric biosensor signal, in the clinically useful range <1 mM sarcosine, especially since the K_m is >10 mM. An amperometric biosensor model was fitted to experimental data to investigate dynamic range. mSOx constructs were designed with 6H (6×histidine) and R5 (silaffin) peptide tags and compared with native mSOx. Glutaraldehyde (GA) cross-linked proteins retained ~5% activity for mSOx and mSOx-6H and only 0.5% for mSOx-R5. In contrast R5 catalysed biosilification on (3-mercaptopropyl) trimethoxysilane (MPTMS) and tetramethyl orthosilicate (TMOS) particles created a 'self-immobilisation' matrix retaining 40% and 76% activity respectively. The TMOS matrix produced a thick layer (>500 µm) on a glassy carbon electrode with a mediated current due to sarcosine in the clinical range for sarcosinemia (0–1 mM). The mSOx-R5 fusion protein was also used to catalyse biosilification in the presence of creatinase and creatininase, entrapping all three enzymes. A mediated GC enzyme linked current was obtained with dynamic range available for creatinine determination of 0.1–2 mM for an enzyme layer ~800 nm.

Keywords: Engineered protein · sarcosine, sarcosine oxidase · biosensor, silaffin · amperometric · thick-film model

1 Introduction

Recently there have been fewer innovations in amperometric enzyme biosensors, possibly because the core idea and technology is robust or perhaps because target analytes with "block buster" applications like the glucose biosensor have not been found. Nevertheless, there are new challenges to overcome with different analytes and in different measurement environments. For example, in low and middle income countries (LMICs), where the burden of chronic non-communicable disease (NCD) is also a challenge. Mainly cardiovascular diseases, diabetes, chronic lung disease and cancers, account for 86% of premature deaths in LMICs [1]. Often there is an absence of even basic functional diagnostic equipment [2,3]. In Mozambique, for example it is reported that only 6% of facilities could carry out a basic blood glucose analysis and personal monitoring is not available in general [4].

Despite good intentions to make technology affordable, costs are exacerbated by the lack of global Purchasing Power Parity for available health technologies, that are almost always imported from richer nations. Thus, local high cost (as a proportion of local income) remains a barrier to diagnostics in LMICs. A joint statement in May 2016 by WHO, UNIDO, UNCTAD, UNAIDS, UNICEF and The Global Fund promoted local production of health technologies to overcome this inequality [5]. The rationale presented is that by bringing the production technology to rural areas, it could develop local economy and improve education, while reducing the cost of technology to the LMIC. This is a multifaceted problem that challenges the entire supply and value chain for a diagnostic. For example, the cost of the enzyme in enzyme linked biosensors, as a component, can account for 70–85% of the total cost invested in many LMICs. Thus, innovation to develop enzymes that can be manufactured locally, specifically for biosensors is in tune with the Sustainable Development Goal (SDG) of Good health and Welbeing as well as having potential to impact SDGs 11 and 8.

We have previously reported a generic approach to engineer and produce many enzymes in low resource environments, for diagnostics [6]. This has been successfully transferred to laboratories in LMICs and, for example, nucleic acid amplification studies have been undertaken in malaria regions and colorimetric and fluorescent biosensors have been studied [6], but there is still much scope to simplify designs and further reduce cost and complexity. Furthermore, although there is also a

[a] S. Chen, E. A. H. Hall
Department of Chemical Engineering and Biotechnology, University of Cambridge, Philippa Fawcett Drive, Cambridge, CB3 0AS, UK

Supporting information for this article is available on the WWW under https://doi.org/10.1002/elan.202000032

clear need, in chronic disease diagnostics, for locally produced glucose test strips, many other metabolites also need to be readily detected and the challenge is to be able to take a common approach that can provide the materials for diagnostics for many different biomarkers. There are numerous examples where new effort is required to allow low cost diagnostics to be a reality in LMICs.

In the work reported herein, we will focus on sarcosine (N-methylglycine), which first gained research interest in a complex 3-enzyme system, where monomeric sarcosine oxidase (mSOx) was found to be useful for the enzymatic determination of creatinine. This could potentially lead to a point-of-care (POC) biosensor for serum creatinine level detection. Creatinine is a metabolic byproduct, and it is an important clinical analyte for the diagnosis and medical management of renal and muscular dysfunction [7,8]. However, this creatinine determination requires a complex three-enzyme system with the sarcosine the penultimate product linked to mSOx, the final enzyme in the cascade. The latter catalyses the oxidative demethylation of sarcosine and forms hydrogen peroxide (which can be measured).

Although sarcosine is not necessarily the most important analyte for LMIC use, it provides a good model for research since, unlike the glucose enzymes, mSOx shows a very low activity and will thus be more representative of the 'real' challenge than the robust glucose enzymes. Furthermore, other health conditions also require direct information about sarcosine levels; sarcosinemia for example, occurs due to a metabolic deficiency of folate, which is required for conversion of sarcosine to glycine. It can result in sarcosine levels $>1000\mu$mole/mmole in urine [9] and plasma levels of 1 mM have been detected in infants, where screening can enable early management. Importantly, sarcosine has also been implicated in the urine of cancer patients, where significantly elevated levels have been recorded in some studies, for patients with prostate cancer (*e.g.* ~1–3 μM in healthy individuals compared with 9–15 μM in patients with prostate cancer) [10]. There is not a consensus on the possible role of sarcosine, but some studies have suggested that sarcosine accumulates in the tumor and exhibits a stimulatory effect on growth in malignant/metastatic prostate cells due to its conversion to serine and glycine [11–13].

In previous studies [6,14] looking at mSOx production for resource poor areas, we reported a sarcosine oxidase fusion enzyme, with mCherry (fluorescent protein) and the silaffin peptide, R5 (H-SSKKSGSYSGSKGSKRRIL-OH). R5 is derived from a naturally occurring silaffin protein that is found in the silica skeleton of the marine diatom Cylindrotheca fusiformis [15,16]. Inclusion of R5 in the fusion, $R5_2$-mCherry-SOx-R5-6H, gave the protein an affinity to silica and enabled it to be isolated directly on silica derived from beach sand. This avoided complex isolation and purification steps. The enzyme remains immobilised on silica and can be used in various diagnostic formats including a novel hour-glass like sensor [6]. These efforts have been directed to optical biosensors, configured as a two enzyme system with horseradish peroxidase and a dye, ultrared. Sarcosine levels could be estimated in the required clinical range for a prostate cancer diagnostic ($<20\,\mu$M) and a preliminary test of urine samples was undertaken [14].

An amperometric biosensor could remove the need for the peroxidase and indicator dye, and further simplify the diagnostic, although detection of such low levels is challenging. Amperometric SOx biosensors have already been reported, mainly using thick film techniques like screen printing [17] or with the inclusion of nanoparticles or porous materials, increasing the surface area for bound enzyme [18]. Surface area for immobiisation and the amount of enzyme required is important for this diagnostic because of the low activity on SOx.

For example, glucose oxidase (GOx) and PQQ-glucose dehydrogenase (GDH) are among the most robust enzymes discovered. The high activity of GOx and GDH has made them ideal candidates as the model enzymes for electrochemical technique development. GOx has a specific activity ranging from 172–300 U/mg (μmol/min/mg) [19,20] and for the non-glycosylated GOx−6H reported in our previous work, the specific activity was 220 U/mg, whereas the enzymatic activity of GDH can be as high as 2000 U/mg. These high activities infer a homogeneous electron transfer rate between the monolayer enzyme and substrate that lead to measurable electrode currents. In contrast, SOx (10–20 U/mg) and other low activity enzymes produce little current for the same amount of enzyme. As shown by Zhou et al. [21], large amounts of enzyme are required to get an equivalent signal. If this is achieved by increasing the electrode surface area, it usually comes with a very high capacitive (background) current.

So, the challenge is to immobilize sufficient enzyme in the vicinity of the electrode to generate an amperometric signal with such a low activity enzyme and be able to measure in the 0–1 mM range (sarcosinemia) or 0–30 μM range (prostate cancer). We have previously reported immobilization of 33 pmole/cm^2 of a C-terminal hexahistidine engineered glucose oxidase (GOx-C6H), at a copper complexed NTA electrode, which was able to produce sufficient current to measure glucose concentrations in the physiological range [22]. In context Zhou et al. [21] needed 118 nmole/cm^2 SOx at an electrode. They achieved this by producing a high surface area for immobilisation with a graphene, chitosan and silver nanoparticle (AgNPs) modified glassy carbon electrode. Despite this success, the oxidation of sarcosine by SOx was not reported, only the (reverse) reduction of its co product, hydrogen peroxide.

The work reported herein targets the sarcosine levels required in the clinical range for sarcosinemia (nominally <1 mM) and considers whether the mSOx-R5 fusion protein provides a self-immobilising protein model that would give access to amperometric enzyme biosensors for low activity enzymes like SOx-6H.

2 Experimental

2.1 Materials

Glutaraldehyde solution 25 % (v/v), Bradford Reagent, sodium chloride, potassium chloride, sarcosine, commercial mSOx, 4-aminoantipyrine, phenol, horseradish peroxidase, sarcosine, ethanol, horseradish peroxidase (HRP), sodium hydroxide (NaOH), hydrochloric acid (HCl), urea, Tetramethyl orthosilicate (TMOS), (3-mercaptopropyl) trimethoxysilane (MPTMS), ferrocene carboxylic acid, potassium chloride, 30 % (v/v) hydrogen peroxide solution, creatininase (E.C. 3.5.2.10), creatinase (E.C. 3.5.3.3), were purchased from Sigma Aldrich. Carbon nanotubes were kindly provided by Alphasense Ltd. Glassy carbon electrode (GCE), silver silver chloride reference electrode (Ag/AgCl) and platinum counter electrode were purchased from BASi, Mineral, Chemistry, Environmental Protection Laboratory Equipment and Harvard Apparatus Ltd respectively.

2.2 Protein Design and Expression

The original mSOx sequence was ordered from GeneArt ™ Gene Synthesis. The gene was cloned into a pEt24a plasmid and expression and isolation followed the procedure described previously [6]. After expression and purification, C-terminal 6H tagged (mSOx-6H) and C-terminal R5 tagged mSOx (mSOx-R5), each gave a yield of 35 mg/L culture. Circular dichroism was carried out in the Department of Biochemistry, University of Cambridge.

2.3 MPTMS Silica Nanoparticles

MPTMS silica nanoparticles were synthesised by vigorously stirring 80 mL DMSO, 3 mL MPTMS, 2 mL of 5 M NaOH, and 120 µL H_2O_2 in a conical flask at room temperature for 24 h. After 24 h of incubation at room temperature, the turbidity of the solution increased, indicating that the particles had been formed. The synthesised MPTMS silica nanoparticles were collected by centrifugation at 13,000 rpm for 10 mins. The MPTMS nanoparticles were then washed 3 times in H_2O, by suspending the collected MPTMS nanoparticles in 1 mL H_2O followed by centrifugation at 13,000 rpm for 10 mins.

2.3.1 Immobilisation of Protein-MPTMS on Gold Electrodes

Protein immobilisation was achieved by vigorously shaking 500 µL protein solution (5 mg/mL) with 100 µL of MPTMS nanoparticles for 2 h, followed by centrifugation at 13000 rpm for 10 min to collect the protein immobilised MPTMS nanoparticles (Protein-MPTMS). Bradford assay was used to determine protein concentration in the supernatant. The loosely bonded protein was removed from the protein-MPTMS composite by washing at least 3 times in 500 µL sodium phosphate buffer (10 mM, pH 7.5). The washed protein-MPTMS was re-suspended in 500 µL sodium phosphate buffer (10 mM, pH 7.5) and the amount of the immobilised protein was determined by subtracting the amount of the protein determined in the washouts from the total amount of the protein (5 mg/mL) that was initially incubated with the MPTMS nanoparticles.

The morphology of MPTMS nanoparticles was examined using scanning electronic microscopy (SEM), and the elements were characterised using Energy-dispersive X-ray spectroscopy (EDX). The hydrodynamic size of MPTMS nanoparticles were characterised by dynamic light scattering (DLS); the mean hydrodynamic diameter for freshly made MPTMS nanoparticle in DMSO was 65 ± 17 nm. After the washing steps, the MPTMS nanoparticles tended to aggregate in the buffer solution; the hydration shell increased the average hydrodynamic diameter to 396 ± 68 nm.

100 µL of the Protein-MPTMS suspension solution was dropped on the gold electrode surface and left at room temperature for 1 h until the buffer was evaporated. Different amounts of protein loading were achieved by diluting the Protein-MPTMS stock solution and the volume of loading was kept the same.

2.4 mSOx-R5 Catalysed TMOS Nanosphere Synthesis

500 µL of mSOx-R5 (5 mg/mL) in 10 mM sodium phosphate buffer pH 7.5 was first concentrated to 20 µL in a Generon Vivaspin 500 concentrating column. A template for TMOS coating was created with a homogeneous CNT suspension, prepared by sonicating CNT (2 mg) in 1 mL sodium phosphate buffer (10 mM, pH 7.5). The silica precipitation reaction mixture on the CNT template consisted of 20 µL of the CNT, 20 µL of the concentrated mSOx-R5 and various amount 20 µL of TMOS precursor solution (1 M in 1 mM HCl). The silica precipitation mix was then vortexed for 5 min. The mSOx-R5-TMOS silica matrices was washed multiple times before use until there was no enzyme detected in the supernatant solution, the final mSOx-R5-TMOS washed matrix was re-suspended in 1 mL of sodium phosphate buffer and the concentration of the immobilised mSOx-R5 was determined using Bradford assay to estimate the binding efficiency.

The surface morphology was visualised using SEM equipped with an energy-dispersive X-ray spectrometer. The microscope was operated at 5.00 kV for imaging. The hydrodynamic size of the mSOx-R5-TMOS matrix was determined using DLS.

The 20 µL of mSOx-R5-TMOS as described above was dropped on the GCE surface. The electrode was left at room temperature for 30mins until the buffer was evaporated. The functionlised electrode was rinsed with sodium phosphate buffer (pH 7.5, 10 mM) prior use.

2.5 Construction of Creatinine Biosensor

20 µL of 25 mg/mL mSOx-R5 in 10 mM sodium phosphate buffer pH 7.5 was mixed with 20 µL of protein solution in the same buffer containing 30 mg/mL creatininase and 50 mg/mL creatinase, followed by adding 20 µL of CNT template suspension solution and (5–20 µL) of 1 M TMOS (in 1 mM HCl). The protein TMOS mixture was vortexed for 10 min at room temperature for the formation of mSOx-R5-creatininase-creatinase-TMOS-CNT matrix. The matrix was then washed three times using 10 mM sodium phosphate buffer pH 7.5 and dropped on the GCE for electrochemical experiments.

2.6 Enzyme Assays for Determination of Kinetic Constants

0–10 µL volumes of sarcosine solution (100 µM), 10 µL of HRP (0.4 mg/mL) and 10 µL of AR (100 mM) were added to 5 mg of already prepared mSOx-construct suspended in water. The final volume in each tube was adjusted to 100 µL with water. After reaction for 20 min at room temperature (in dark) the fluorescence was measured at excitation/emission wavelength 530/582 nm. The increment of fluorescence intensity of sarcosine standard (I_{Sar}) with respect to the blank (I_0) was plotted against the concentration of sarcosine.

A Bradford assay was used to determine total protein (active and non active). 20 µL of protein solution was added to 100 µL Bradford reagent (Coomassie Brilliant Blue in phosphoric acid) in a well plate and absorbance at 595 nm was measured with a UV spectrophotometer and compared with a standard curve made with BSA.

Electrochemical data were recorded using a PSTAT 10 Autolab potentiostat (Eco-Chemie).

2.7 Theoretical Modelling of the Mediated Amperometric Biosensor Response

The mathematical model developed previously by us [23,24] for enzyme film layers in the amperometric enzyme electrode, was used to compare the current response of different mSOx biosensor constructs. The reaction mechanism of the enzyme follows a mediated Ping-Pong mechanism as refered to later in section 3.2, where the model is described. The derivation and general assumptions were as reported previously with the following boundary condition created by the second generation redox mediator, ferrocene carboxylic acid (FCA): reduced mediator (Med_{red}) was provided to the system in bulk solution. Normalised reduced mediator concentration $[Med_{red}]=0$ at the electrode and $[Med_{red}]=1$ at the enzyme layer solution interface. The 'active' form of the mediator for reoxidation of the enzyme is $[Med_{ox}]=1-[Med_{red}]$. The highest concentration of Med_{ox} will be in a zone next to the electrode. The current (measured at 0.4 V versus Ag/AgCl) arises from the flux of $[Med_{red}]$ at the electrode.

3 Results and Discussion

3.1 Performance of Peptide Tagged SOx

Monomeric sarcosine oxidase (42 kDa) originates from *Bacillus sp.* It is a two-domain protein, with the FAD making contact with side chains of arginine, lysine, histidine and the N-terminal end of a helix dipole and creating an alkaline environment. The isoalloxazine ring complex (IRC) of FAD is covalently attached to the Cys315 of the catalytic domain through an 8α-S-cysteinyl linkage [25,26]. Substrate binding is believed to be located above the *re* face of the IRC ring, stabilised by hydrogen bonds between the substrate carboxylate and the two basic side chains, Arg52 and Lys348. The adenine ring of FAD lies at 23.542 Å from the C-terminus, which is slightly less than the distance from the N terminal (25.89 Å). There is no indication from this structure that engineering of the C terminal of the enzyme should strongly influence the enzyme activity, so to design SOx constructs suitable for forming a thick enzyme layer on the electrode to produce a functional amperometric biosensor, with a low activity enzyme like mSOx, two basic recombinant enzyme constructs were synthesised, with C terminal modification of mSOx: mSOx-6H, having a hexa-histidine peptide tag and mSOx-R5, having a silaffin tag. In solution, the engineered and native enzymes had a similar K_m but higher k_{cat} was observed for the engineered enzymes than the native enzyme (Table 1), suggesting that there had been no detrimental effect on the active site through C terminal modification. Circular Dichroism (CD) and structure modelling (supplementary data Figure S1 and Table S1) are also consistent with there being no major change in the basic mSOx enzyme folding.

3.2 Glutaraldehyde Immobilized Enzyme Performance

In preliminary enzyme electrode research, enzyme layers have often been formed using glutaraldehyde (GA) crosslinking. Adopting this approach here (Figure 1a) resulted in considerable loss in enzyme activity. Compared with the enzyme prior to crosslinking, only ~5% activity remained for the mSOx-GA and mSOx-6H-GA and only

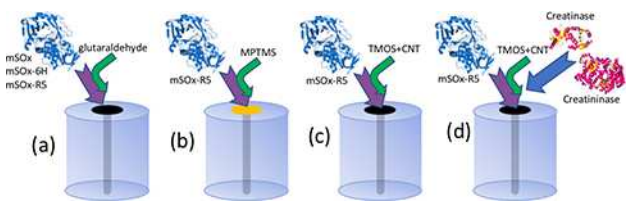

Fig. 1. Cartoon of enzyme immobilisation for mSOx and its peptide constructs. (a) glutaraldehyde crosslinking of mSOx, mSOX-6H and mSOx-R5. (b) MPTMS silanisation with mSOx-R5 on an Au electrode. (c) TMOS silanisation with mSOx-R5 with a CNT template. (d) as for (c) with creatinase and creatininase added. Enzyme structures drawn from the RCSB Protein Data Bank.

Table 1. Parameters in the enzyme layer model and comparison of enzyme kinetic values for mSOx, mSOx-6H and mSOx-R5.

	mSOx		mSOx-6H		mSOx-R5	
	In solution	GA crosslinked	In solution	GA crosslinked	In solution	GA crosslinked
Residual activity (%)	100	5.0 ± 0.4	100	5.6 ± 0.5	100	0.5 ± 0.1
K_m (mM)	16.1	13.5	16.3	12.9	16.5	15.3
k_{cat} (s^{-1})	9.7	2.67×10^{-3}	12.4	3.56×10^{-3}	16.7	2.81×10^{-4}
k^*_{cat} (s^{-1})	N/A	5.34×10^{-3}	N/A	7.12×10^{-3}	N/A	5.62×10^{-3}
k_s ($M^{-1}s^{-1}$)	–	$0.48 \pm .03 \times 10^4$	–	$0.66 \pm 0.05 \times 10^4$	–	$0.07 \pm 0.09 \times 10^4$
k^*_s ($M^{-1}s^{-1}$)	–	$9.6 \pm 0.6 \times 10^4$	–	$11.8 \pm 0.7 \times 10^4$	–	$15.0 \pm 1.6 \times 10^4$
$[E_T]^*$ (mM)	–	1.29	–	0.83	–	0.12
$[Med]_b$ (mM)	–	1	–	1	–	1
(D_m) (cm^2/s)	–	8.5×10^{-6}	–	8.5×10^{-6}	–	8.5×10^{-6}
(D_s) (cm^2/s)	–	5.5×10^{-6}	–	5.5×10^{-6}	–	5.5×10^{-6}
(d) (μm)	–	315	–	328	–	401
A (cm^2)	–	0.256	–	0.256	–	0.256
ϕ^2	–	8.07×10^{-5}	–	7.48×10^{-5}	–	1.28×10^{-5}

$[E_T]^*$, k^*_{cat} and k^*_s are adjusted for *active* enzyme. D_m and D_s are diffusion coefficients for the mediator and substrate respectively. E_T refers to total enzyme concentration added. A is electrode area, d is enzyme layer thickness. K_m and k_{cat} in solution are calculated from the method in 2.6. The kinetic constants for the immobilized enzyme were obtained by fitting the experimental data to the electrochemical form of the Michaelis-Menten equation where reaction velocity is replaced by current (Figure 2A2, 1B2 and 1C2

0.5 % for mSOx-R5-GA (Table 1). Despite this, using a second generation mediator like ferrocene dicarboxylic acid (FCA), SOx enzyme electrodes gave a measurable current response to sarcosine. However, it can be seen visually in Figure 2.A1, 2.B1, 2.C1 that the GA cross linking results in a different electrode performance for each enzyme. Mediator (FCA) catalysis was confirmed from the plot of $i_p/v^{1/2}$ vs. log(scan rate, v) and the kinetic parameter (k_f/a) was extracted, using the theoretical plot derived by Nicholson and Shain [27] (Figure 2.A3; 2.B3 and 2.C3). This enabled the value of k_f (pseudo first order rate constant) to be obtained from the slope of the plot and thence the homogeneous second-order rate constant ($k_{s=} = k_f/[mSOx]$) for FCA in the electrode construct. Taking into account the deactivation of the enzyme by GA cross-linking (Table 1), the values for k^*_s obtained for ferrocene dicarboxylic acid as mediator with mSOx and mSOx-6H were an order of magnitude lower than for glucose oxidase and required at least 20x more enzyme to achieve a measurable current. Furthermore, since the K_m is circa 16 mM, measurement targeting plasma sarcosine levels associated with sarcosinemia (<1000 μM) will be at the low end of the calibration curve, where sensitivity will be more challenging.

The chronoamperometric data at different sarcosine concentrations (Figure 2.A2, 2.B2, 2.C2) showed slightly lower K_m than in solution, but consistent with an enzyme that has retained its structural activity (Table 1). The electrochemically derived value for k^*_{cat} was also of the same order for the three enzymes.

In thick enzyme layer electrodes, the layer properties can affect the response and dynamic range of the enzyme. From the mathematical models developed by us previously [23,24], for an enzyme electrode, diffusion and reaction in the enzyme layer are important in determining the electrode current and the available dynamic range. This can be categorised according to the thiele modulus, $\phi^2 = (d^2 k_{cat}[E_T])/(D_{med}[Med]_b)$. When ϕ^2 is small, the response of the sensor is limited by the enzyme kinetics and when ϕ^2 is large it is limited by transport of substrate and mediator to the enzyme. Taking the kinetic parameters from the Michaelis Menten fit in Figure 2 as input values, changes affecting ϕ^2 can be further explored. The model is illustrated in Figure 3a, where the mediator FDA is supplied in its reduced state (Med_{red}) and is oxidised at the electrode to the ferrocenium ion (Med_{ox}). At the applied oxidising potential $[Med_{red}] = 0$ at the electrode surface and $[Med_{red}] = 1$ at the enzyme layer/solution interface.

To understand this in the context of the SOx layers produced by GA crosslinking, the calibration curves obtained at the GCE-mSOx-GA, GCE-mSOx-6H-GA and GCE-mSOx-R5-GA were fitted to the model (Figure 3b). The layer thickness was estimated from SEM images and was similar for all these electrodes (354 ± 51 μm). This is unsurprising since the same mass (but not activity) of enzyme and GA were used in each case. Diffusion coefficients for substrate and mediator were not adjusted for the matrix, but were taken from the literature. It is noted that the predicted $\phi^2$is similar and small in all cases (Table 1), indicating that the response at the electrode is limited by enzyme kinetics.

Despite adding the same amount of enzyme to each electrode for GA cross-linking, the amount of active enzyme was particularly influenced by the R5 peptide affinity tag, possibly as a result of the number of positively charged amino acids in the tag (SSKKSGSYSGSKGSKRRIL) that are ideal for cross-linking with glutaraldehyde. As a result, the residual SOx activity might be affected by the protein engineering; fitting the curves in Figure 3b to the model predicts 1.29, 0.83 and 0.12 mM enzyme for GCE-mSOx-GA, GCE-mSOx-6H-GA and GCE-mSOx-

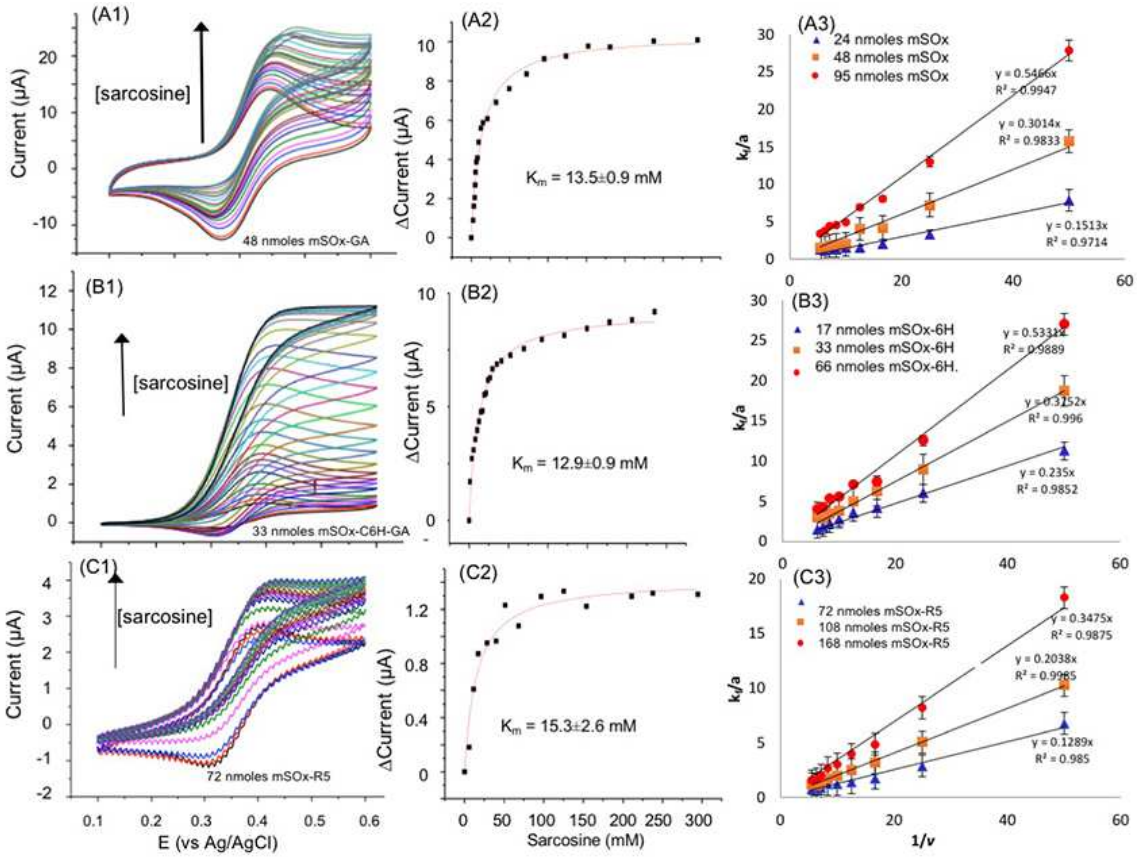

Fig. 2. Cyclic voltammograms of A1: 48 nmoles of mSOx-GA, B1: 33 nmoles of mSOx-6H-GA, C1: 72 nmoles of mSOx-R5-GA modified GCE at various sarcosine concentrations as given in figures A2, B2 and C2 respectively. CV were recorded at scan rate of 50 mV/s. Current response from chronoamperometry of, A2 (21 data sets in duplicate), mSOx-GA, B2 (21 data sets in duplicate), mSOx-6H-GA and C2 (14 data sets), mSOx-R5-GA at a GC electrode at 0.4 V for various sarcosine concentrations. All data points are plotted; note that some points overlap and are not resolved. The experimental errors were calculated from the curve fitting. Plots of kinetic parameter k_f/a vs. 1/v for the reaction of FCA at, A3, mSOx-GA; B3, mSOx-6H-GA and C3, mSOx-R5-GA. The data was obtained from cyclic voltammetry carried out in 10 mM sodium phosphate buffer pH 7.5 containing 50 mM KCl, 300 mM sarcosine. The values of k_f/a were obtained from a working curve derived by Nicholson and Shain [27], and $a = nF\,v/RT$. All data were recorded in 1 mM FCA with various concentrations of sarcosine in 10 mM phosphate buffer containing 50 mM KCl pH 7.5. Ag/AgCl was used as the reference electrode and platinum was used as the counter electrode.

R5-GA electrodes respectively (see Table 1). Taking the enzyme layer thickness as the same in each case, the curves in figure 3b suggest that [ET] interpreted as active enzyme, dominates the differences in the plots, so that GCE-mSOx-R5-GA (with circa 10 % active enzyme compared with GCE-mSOx-GA) has the lowest current response.

This provides an experimental basis to explore the effects of layer thickness and active enzyme loading further. Figure 3c shows the predicted variation in current change with the concentration of sarcosine, modelled for various values of *d*, with constant enzyme loading and enzyme kinetics. These plots show a reduced dynamic range as the thickness increases. This is accompanied by an increase in ϕ^2 and arises because the active Med_{ox} is generated at the electrode and, for enzyme layers thicker than the diffusion layer thickness a concentration gradient extends from $[Med_{ox}] = 1$ at the electrode to $[Med_{ox}] = 0$ at distance x' within the layer. This determines that the oxidation of the enzyme by Med_{ox} is confined to the zone between $0 < x > x'$. Since, the detection range is limited by the available Med_{ox}, the signal may saturate at artificially low sarcosine concentration. For a low activity enzyme like SOx, targeting a low dynamic range which is circa 10 % of its K_m this reduced range is not problematic. Indeed, the increase signal resolution within that range is an advantage. Since ϕ^2 also shows a linear dependence on $[E_T]$, enzyme concentration will have a lesser but still important effect on the usable concentration range of the sensor, compared with the squared relationship for thickness. For example, for a constant thickness of 200 μm, Figure 3d suggests that the dynamic range will become limited ~2 mM SOx in the enzyme layer.

From the trends in Figure 3d and c both active enzyme $[E_T]$ and layer thickness *d* need to be increased to gain the required sensitivity at low sarcosine concentrations. To approach this problem, advantage was taken of the R5 peptide fused SOx, which was used directly to precipitate

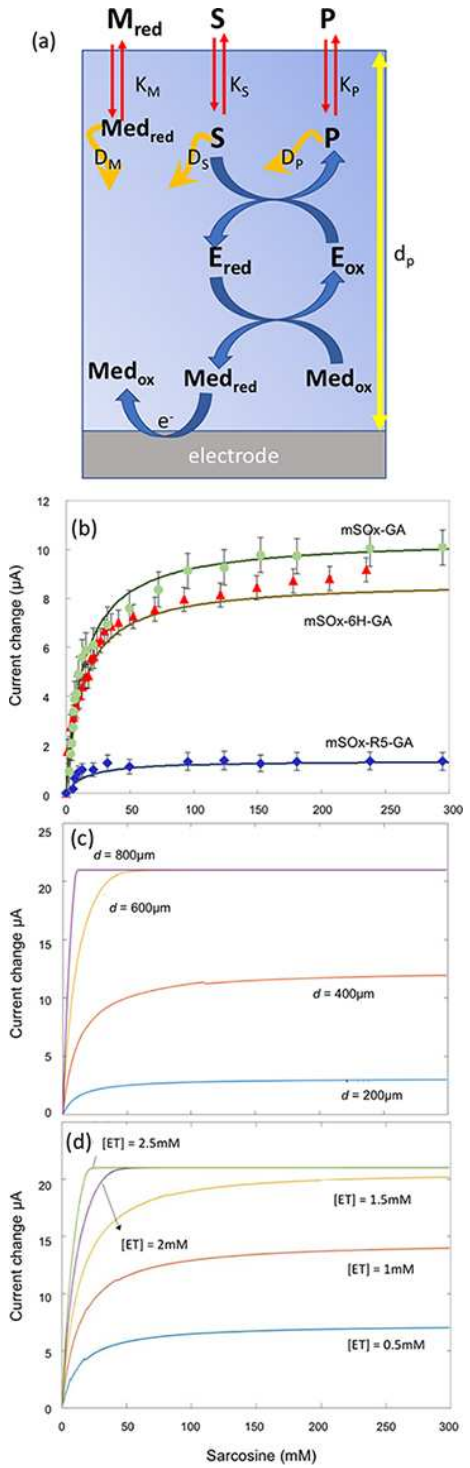

Fig. 3. (a) Scheme for the thick layer mediated amperometric SOx electrode. (b) Experimental data and model fit, for current response at different sarcosine concentration for mSOx-GA, mSOx-6H-GA and mSOx-R5-GA. Model predictions for variation in sensor current with sarcosine concentration for different values of (c) d (enzyme loading was constant at 0.2 mM) and (d) $[E_T]$ (thickness was kept at constant at 200 μm) The mediator concentration was 1 mM.

an enzyme layer, without requiring additional coupling reagents and with higher enzyme activity.

3.3 Silica Immobilized Enzyme Performance with R5 Peptide

As reported previously [6], the R5 peptide was designed for easy isolation of the recombinant protein on silica isolated from beach sand and then subsequent use of the enzyme, still attached to the sand. By adding the R5 sequence to the protein construct, the positively charged residues on the R5 polypeptide (K and R) [28] will interact with the negative charge of the silica surface.

The use of particulate silica, allows a layer to be created, supported by the particle. As particle size increases, the surface area to volume ratio decreases and thus the immobilisation efficiency per weight of silica decreases, although packing density and diffusion through the void volume will also influence the kinetics. To take this silica (sand) immobilisation process further, tetramethyl orthosilicate (TMOS) derived particles were used for initial study rather than beach sand.

The silica obtained from beach sand is a heterogeneous size and non-spherical population (figure 4c), so to partially simulate this with a more controlled sample, two populations of particles were produced: <1 μm particles that were approximately spherical, and particles of 300–800 μm long dimension (Figure 4b) that were seeded onto CNT templates to make them non-spherical. Unfortunately, enzyme modified TMOS particles <1 μM did not form a stable layer on the GCE electrode, so (3-mercaptopropyl) trimethoxysilane (MPTMS) derived particles (Figure 1b and 4a) were used on a gold electrode. This formed a stable layer, possibly through coupling to the gold via the thiol group. Figure 4c shows the hydrodynamic radius obtained by dynamic light scattering, for the different particles, confirming the size difference and also comparing the TMOS coated particles to the silica derived from sand that we have used previously for enzyme immobilization. The SEM images (Figure 4a and 4b) of the resultant particles after deposition confirm the different shapes and suggest a more densely packed matrix arises from the small MPTMS particles.

SOx immobilization on the MPTMS particles was 85 % efficient, below saturating concentrations, based on the colorimetric activity assay (see Materials and Methods) and the resultant enzyme-MPTMS layers gave an apparent specific activity of 8.6 ± 1.1 U/mg adsorbed protein. This is 40 % of the specific activity for mSOx-R5 in solution, but it isn't clear whether the loss is due to loss of activity of the protein (eg thiol coupling between MPTMS and the protein) or reduced accessibility. Our previous work has shown that depending on the porosity or packing of silica particles, not all immobilized enzyme is accessible to the substrate/solution [6].

In contrast the larger TMOS coated particles (Figure 1c) achieved similar immobilization efficiency but recorded 76 % of the specific activity in solution. A

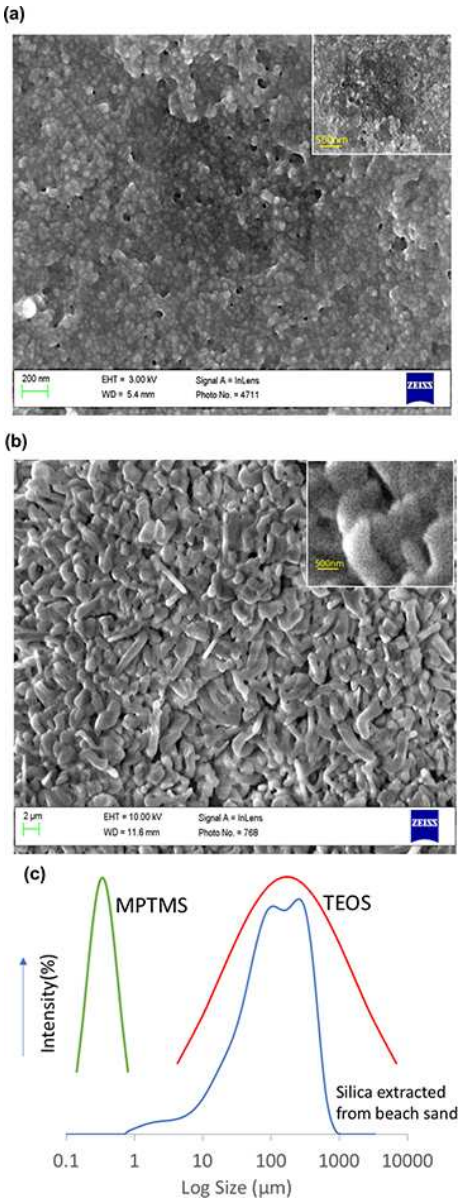

Fig. 4. SEM image of (a) mSOx-R5-MPTMS matrix (b) mSOx-R5-TMOS matrix. (c) Hydrodynamic size distribution of mSOx-R5-MPTMS matrix and mSOx-R5-TMOS matrix (10 mM in sodium phosphate buffer) compared with silica extracted from beach sand.

suspension of the enzyme modified particles was dropped onto the electrode and dried to create a film of $d = 315 \pm 38$ µm and 740 ± 63 µm for the MPTMS and TMOS particles respectively (measured from SEM data). The cyclic voltammogram for 1 mM FCA produced the characteristic mediated current in the presence of sarcosine (Figure 5a,d). Analysis of $i_p/v^{1/2}$ vs. log(v) showed $i_p/v^{1/2}$ decreasing with scan rate, consistent with a catalytically controlled reaction as before. This leads to a second order rate constant k^*_s for the mediator kinetics derived from k_f, obtained from the slope of the lines in Figure 5c and 5f, which yielded similar values to those obtained for the glutaraldehyde cross linked electrodes (see Table 2). This is expected for the same mediator and enzyme.

The chronoamperometric data for these electrodes, at different sarcosine concentrations gave calibration curves (Figure 5b,e) that could be fitted to the Michaelis Menten relationship to derive the apparent K_m and k_{cat} of the immobilised mSOx-R5. The estimates obtained from these fits yield an apparent K_m for the mSOx-R5 in MPTMS of 3.9 ± 0.6 mM and 4.2 ± 0.17 mM on TMOS (Table 2). However, despite the apparently good fit, visual inspection of these data in Figure 5b,e suggests that the dynamic range is limited and the data are reaching 'saturation' currents. Thus, these data were fitted to the model for a enzyme layer system (Figure 6) to explore their performance compared with GCE-mSOx-R5-GA.

The gold-mSOx-R5-MPTMS had a 7-fold increase in active [E_T] (as measured from the activity assay, see section 2.6) but decrease in thickness, compared with the GCE-mSOx-R5-GA. The model for gold-mSOx-R5-MPTMS suggested a decrease in the diffusion coefficient for the mediator in this matrix (Table 2) would account for the increase in diffusion limitation, but similar current response (Figure 6a,b versus Figure 3b). This may be consistent with the apparently dense structure indicated from the SEM in figure 4a. In contrast, the electrodes with the GCE-mSOx-R5-TMOS, have an order of magnitude increase in active [E_T], combined with increase in layer thickness, compared with GCE-mSOx-R5-GA. This resulted in a dynamic range limited to 7 mM sarcosine, but with an increase of 440 % in the current (Figure 6c,d) within the clinical range which would be used for determination of sarcosine. We conclude therefore, that the R5 catalysed biosilification can provide a useful thick layer immobilisation method for mSOx in an amperometric electrode.

3.4 Application in a Multienzyme Model

This approach can also be applied to adjusting the limit of detection and dynamic range for more complex enzyme systems. For example, as discussed in the introduction, creatinine can be measured in the following pathway:

$$\text{Creatinine} + H_2O \xrightarrow{\text{Creatininase}} \text{Creatinine} + H_2O$$

$$\text{Creatine} + H_2O \xrightarrow{\text{Creatinase}} \text{Sarcosine} + \text{Urea}$$

$$\text{Sarcosine} \xrightarrow{\text{mSOx}} \text{Glycine} + \text{Formaldehyde} + H_2O_2$$

In our previous work using cascading enzyme pathways [14], we combined mSOx immobilised on silica with peroxidase immobilised separately, using GA. By co-immobilising creatininase and creatinase with mSOx (Figure 1d), it was possible to generate an optical detection method for creatinine. However, since the R5 tag catalyses the biosilification of tetramethyl orthosilicate (TMOS) [29,30], the mSOx-R5 might be able to catalyse

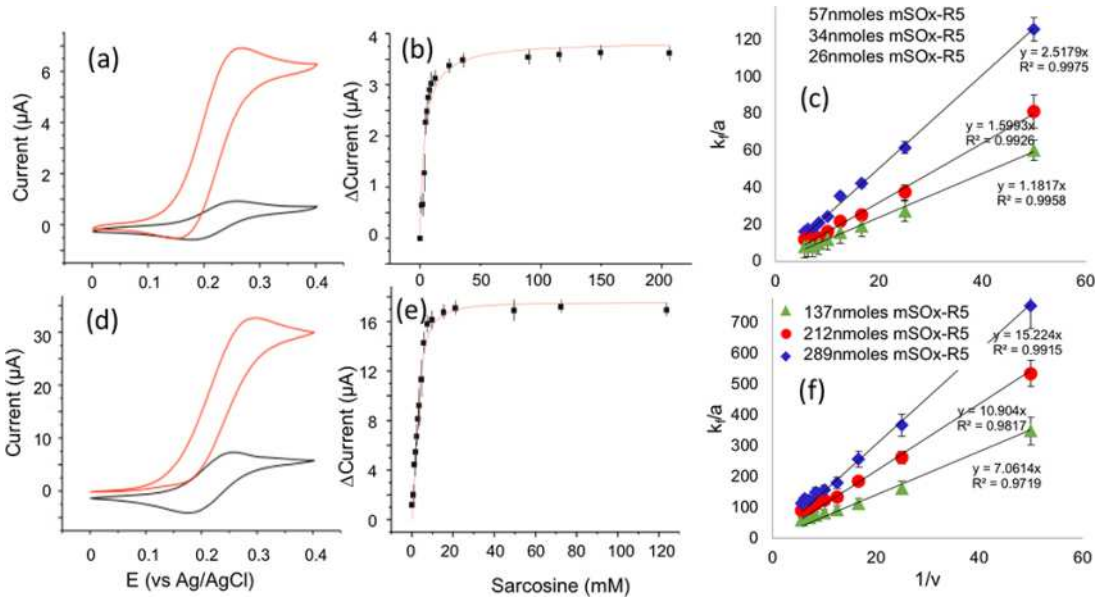

Fig. 5. Cyclic voltammograms of (a) mSOx-R5-MPTMS gold electrode (d) mSOx-R5-TMOS GC electrode containing 1 mM FCA and 0 (black) or 300 mM sarcosine (red). CV were recorded at scan rate of 50 mV/s. Current response from chronoamperometry of (b) mSOx-R5-MPTMS gold electrode and (e) mSOx-R5-TMOS GC electrode at a GC electrode at 0.4 V for various sarcosine concentrations. Plots of kinetic parameter k_f/a vs. 1/v for the reaction of FCA at (c) mSOx-R5-MPTMS gold electrode and (f) mSOx-R5-TMOS GC electrode. The data was obtained from cyclic voltammetry carried out in 10 mM sodium phosphate buffer pH 7.5 containing 50 mM KCl, 300 mM sarcosine. The values of k_f/a were obtained from a working curve derived by Nicholson and Shain [27], and $a = nF\ v/RT$. Ag/AgCl was used as the reference electrode and platinum was used as the counter electrode.

Table 2. Comparison of enzyme kinetic values for GCE-mSOx-R5-TMOS Gold-mSOx-R5-MPTMS and GCE-mSOx-R5-GA.

	GCE-mSOx-R5-TMOS	Gold-mSOx-R5-MPTMS	GCE-mSOx-R5-GA
d (μm)	740	315	401
$k^{\#}_{cat}$(s^{-1})	5.62×10^{-3}	5.62×10^{-3}	5.62×10^{-3}
E^*_T (mM)	1.12	0.89	0.12
D_{med} (cm^2/s)	6.9×10^{-6}	1.0×10^{-6}	8.5×10^{-6}
A (cm^2)	0.233	0.078	0.256
k_s ($M^{-1}s^{-1}$)	$10.2\pm0.12\times10^4$	$3.5\pm1.1\times10^4$	$0.07\pm0.09\times10^4$
k^*_s ($M^{-1}s^{-1}$)	$13.4\pm0.14\times10^4$	$8.75\pm1.2\times10^4$	$15.0\pm1.6\times10^4$

k^*_s is adjusted for *active* enzyme. $k^{\#}_{cat}$ is the input value used in modelling.

the co-entrapment of other native proteins without additional protein engineering. It has been reported that protein activity has been retained with an R5 catalysed entrapment of silica, but Marner *et al.* [31] reported that a simple mixture of R5 with the protein of interest in the 1:1 molar ratio was not capable of silification.

Nevertheless, to test this multienzyme approach the GCE-mSOx-R5-TMOS was produced in the presence of creatininase and creatinase; this produced an enzyme layer thickness of 145 ± 23–900 ± 38 μm. Figure 7a shows that the surface morphology of the mSOx-R5-creatininase-creatinase-TMOS is less uniform than the microsphere structure observed at the mSOx-R5-TMOS. This is probably because the mSOx-R5-creatininase-creatinase-TMOS has encapsulated 2.75 times more protein and created a more protein rich structure. Figure 7b shows the chronoamperometric data in the presence of creatinine for a layer thickness of. From these data and considering the background current, the biosensor gives a limit of detection of 340 μM with dynamic range up to 1430 μM. However the required range of clinical interest for sarcosinemia is from 10 to 1000 μM so the higher concentration response and dynamic range can be sacrificed to obtain higher sensitivity at lower concentration.

Although this multi-enzyme model has not been modelled, from the modelling of the layer thickness discussed earlier for one enzyme, an increase in the thickness might increase sensitivity and decrease range, so the layer thickness was increased by increasing the amount of TMOS in the R5 catalysed biosilification. Figure 7c and d show the FCA mediated current change for enzyme layers of 123–783 μm. These layers are stable with enzyme activity being retained at room temperature

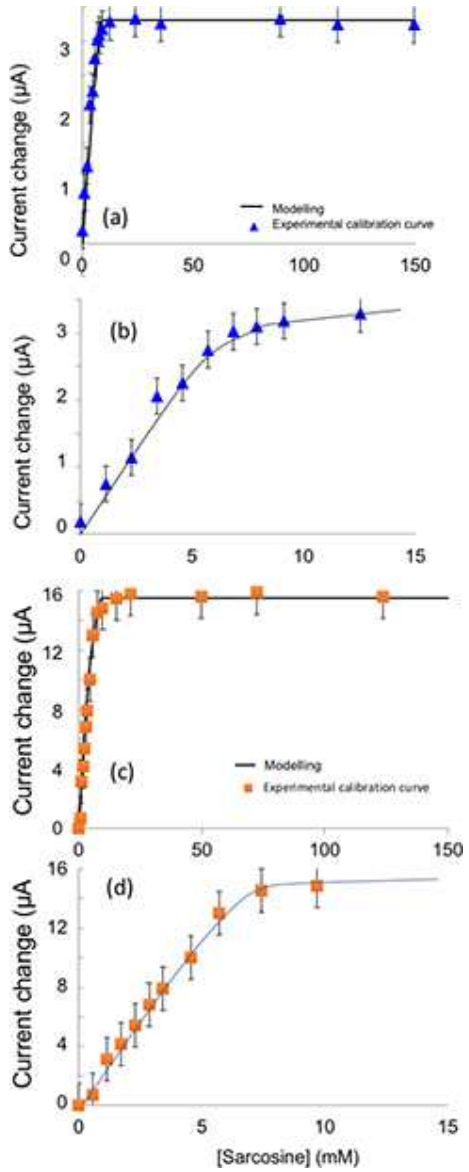

Fig. 6. Fitting the model to experimental data for the current response of (a) and (b) Au-mSOx-R5-MPTMS and (c) and (d) GCE-mSOx-R5-TMOS at various sarcosine concentrations. (a) and (c) sarcosine concentration range: 0 mM–150 mM (b) and (d) sarcosine concentration range: 0 mM–15 mM. Current response was obtained from chronoamperometry at 0.4 V in 10 mM sodium phosphate buffer pH 7.5 containing 50 mM KCl, 1 mM FCA. Ag/AgCl was used as the reference electrode and platinum was used as the counter electrode.

over several weeks (as shown previously [6,14]). For the thickest layer, the LOD is reduced to 8 μM, with a dynamic range to 1700 μM. This has not yet been tested on clinical samples but it demonstrates a considerable increase in versatility of the R5 fusion proteins, where a 'mix and match' combination might be achieved by exploiting the biosilification capabilities of the peptide as well is its ability to adsorb fusion proteins on to silica with high retention of enzyme activity.

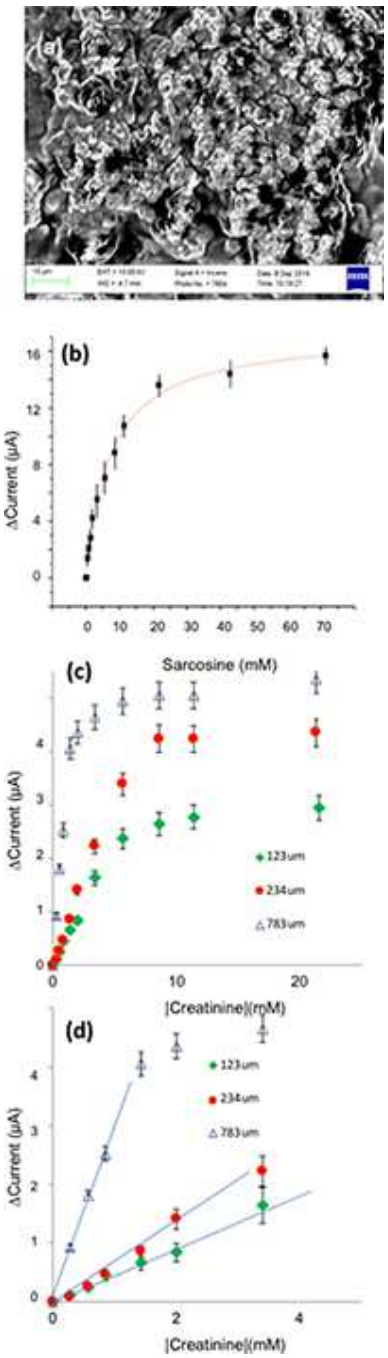

Fig. 7. (a) SEM of the mSOx-R5-creatininase-creatinase-TMOS composite (b) Chronoamperometric responses curve of the GCE-mSOx-R5/creatininase-creatinase electrode (333 μM mSOx-R5)-TMOS electrode. Applied potential: +0.4 V vs Ag/AgCl; counter electrode: platinum; supporting electrolyte: 1 mM FCA,10 mM sodium phosphate buffer, 50 mM KCl pH 7.5. The experimental errors was calculated from the curve fitting. (c) and (d) (scale expanded) comparison of current response at the GCE-mSOx-R5-creatininase-creatinase-TMOS electrode with same enzyme loading, but different layer thickness, achieved by varying amounts of TMOS.

3 Conclusions

In this manuscript we have reported on the further use of the mSOx-R5 fusion protein in creating enzyme layers of variable thickness. Previous work [6] has shown the easy production and isolation of these R5 fusion proteins in a low resource environment due to their affinity for silica, allowing non-denaturing irreversible immobilisation of the protein. Silica is a core low cost abundantly available material which we have obtained previously from beach sand. In this work, we show that the R5 catalysed biosilification can be used to build stable thick enzyme layers and we have applied this technique to the development of a thick layer amperometric enzyme model using monomeric sarcosine oxidase to measure sarcosine. This low activity enzyme is a challenging system for an amperometric biosensor, since not only is its activity only circa 1 % of many of the redox glucose enzymes used in biosensors, but the targeted clinical range is only 10 % of the enzyme K_m. Nevertheless, using a silica matrix for enzyme immobilisation of the R5 fused mSOx, we are able to show how the enzyme layer can be manipulated to obtain a stable thick layer able to produce a measurable current in the required range. Furthermore, the R5 catalysed biosilification system can be further applied to multienzyme systems with unexpected success. In this case, a combination of creatininase and creatinase were co immobilised with mSOx-R5, allowing an enzyme electrode to be produced of ~1 mm thick enzyme layer that responded to creatinine with a LOD of 8 μM, and a dynamic range to 1700 μM. Importantly, this result shows that the biosilification only requires one protein to contain the R5 tag. However, we have previously shown that without the R5, the immobilisation is not stable [6].

The data reported herein provide a basis to further expand the manufacturing techniques for use in low resource areas and to contribute to the challenge of delivering sustainable diagnostics in these environments.

References

[1] WHO Global status report on noncommunicable diseases 2014. *World Health* **2014**: 176. ISBN: 9789241564854.

[2] L. D. Yan, C. Chirwa, B. H. Chi, S. Bosomprah, N. Sindano, M. Mwanza, D. Musatwe, M. Mulenga, R. Chilengi, *BMC Health Serv. Res.* **2017**, *17*, 111.

[3] I. Risso-Gill, D. Balabanova, F. Majid, K. Keat Ng, K. Yusoff, F. Mustapha, C. Kuhlbrandt, R. Nieuwlaat, J.-D. Schwalm, T. McCready, K. K. Teo, S. Yusuf, M. McKee, *BMC Health Serv. Res.* **2015**, *15*.

[4] D. Beran, J. S. Yudkin, M. De Courten, *Diabetes Care.* **2005**, *28*, 2136–2140. doi:10.2337/diacare.28.9.2136.

[5] N. Engel, K. Wachter, M. Pai, J. Gallarda, C. Boehme, I. Celentano, R. Weintraub, *BMJ Global Health* **2016**, *1*, e000132.

[6] C. J. Henderson, E. Pumford, D. J. Seevaratnam, R. Daly, E. A. H. Hall, *Biomaterials* **2019**, *193*, 58–70.

[7] S. Yadav, R. Devi, P. Bhar, S. Singhla, C. S. Pundir, *Enzyme Microb. Technol.* **2012**, *50*, 247–254.

[8] J. A. Weber, A. P. van Zanten, *Clin. Chem.* **1991**, *37*, 695–700.

[9] A. Benarrosh, R. Garnotel, A. Henry, C. Arndt, P. Gillery, J. Motte, S. Bakchine, *JIMD Reports – Case and Research Reports* **2012**, *6*, 93–96.

[10] V. Yamkamon, B. Phakdee, S. Yainoy, T. Suksrichawalit, T. Tatanandana, P. Sangkum, W. Eiamphungporn, *EXCLI Journal* **2018**, *17*, 467–478.

[11] A. P. Khan, T. M. Rajendiran, B. Ateeq, I. A. Asangani, J. N. Athanikar, A. K. Yocum, R. Mehra, J. Siddiqui, G. Palapattu, J. T. Wei, G. Michailidis, A. Sreekumar, A. M. Chinnaiyan, *Neoplasia* **2013**, *15*, 491–501.

[12] Z. Heger, M. A. Merlos Rodrigo, P. Michalek, H. Polanska, M. Masarik, V. Vit, M. Plevova, D. Pacik, T. Eckschlager, M. Stiborova, V. Adam, *PLoS One.* **2016**, *8*, 11, e0165830.

[13] M. A. Merlos Rodrigo, V. Strmiska, E. Horackova, H. Buchtelova, V. Adam, P. Michalek, M. Stiborova, T. Eckschlager, Z. Heger, *The Prostate.* **2018**, *78*, 104–112.

[14] N. Jornet-Martínez, C. J. Henderson, P. Campíns-Falcó, R. Daly, E. A. H. Hall, *Sens. Actuators B* **2019**, *287*, 380–389.

[15] N. Kröger, *Curr. Opin. Chem. Biol.* **2007**, *11*, 662–669.

[16] N. Poulsen, M. Sumper, N. Kroger, *Proc. Mont. Acad. Sci.* **2003**, *100*, 12075–12080.

[17] T. S. Rebelo, C. M. Pereira, M. G. Sales, J. P. Noronha, J. Costa-Rodrigues, F. Silva, M. H. Fernandes, *Anal. Chim. Acta.* **2014**, *850*, 26–32.

[18] H. Yang, J. Wang, C. Yang, X. Zhao, S. Xie, Z. Ge, *J. Electrochem. Soc.* **2018**, *165*, H247–H250.

[19] H. Tsuge, O. Natsuaki, K. Ohashi, *J. Biochem.* **1975**, *78*, 835–43.

[20] C. Simpson, J. Jordaan, N. S. Gardiner, C. Whiteley, *Protein Expr. Purif.* **2007**, *51*, 260–266.

[21] Y. Zhou, H. Yin, X. Meng, Z. Xu, Y. Fu, S. Ai, *Electrochim. Acta* **2012**, *71*, 294–301.

[22] S. Demin, E. A. H. Hall, *Bioelectrochemistry*, **2009**, *76*, 19–27.

[23] J. J. Gooding, M. Hämmerle, E. A. H. Hall, *Sens. Actuators B* **1996**, *34*, 516–523.

[24] J. J. Gooding, E. A H. Hall, D. B. Hibbert, *Electroanalysis* **1998**, *10*, 1130–1136.

[25] A. Han, T. Shibata, T. Takarada, M. Maeda, *Nucleic Acids Res. Suppl.* **2002**, *21*, 287–8.

[26] G. Zhao, H. Song, Z.-W. Chen, F. S. Mathews, M. S. Jorns, *Biochemistry* **2002**, *41*, 9751–64.

[27] R. S. Nicholson, I. Shain, *Anal. Chem.* **1964**, *36*,706–723.

[28] S. V. Patwardhan, F. S. Emami, R. J. Berry, S. E. Jones, R. R. Naik, O. Deschaume, H. Heinz, C. C. Perry, *J. Am. Chem. Soc.* **2012**, *134*, 6244–6256.

[29] H. R. Luckarift, J. C. Spain, R. R. Naik, M. O. Stone, *Nat. Biotechnol.* **2004**, *22*, 211–213.

[30] K. E. Marshall, E. W. Robinson, S. M. Hengel, L. Paša-Tolić, G. Roesijadi, *PLoS One* **2012**, *7*, 1–8.

[31] W. D. Marner, A. S. Shaikh, S. J. Muller, J. D. Keasling, *Biotechnol. Prog.* **2009**, *25*, 417–423.

Received: January 14, 2020
Accepted: March 2, 2020
Published online on ■■, ■■

FULL PAPER

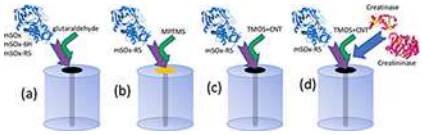

*S. Chen, E. A. H. Hall**

1 – 12

A Biosilification Fusion Protein for a 'Self-immobilising' Sarcosine Oxidase Amperometric Enzyme Biosensor